LAWRENCE
LIVERMORE
NATIONAL
LABORATORY

UCRL-PROC-222562

Highly-resolved 2D HYDRA simulations of Double-Shell Ignition Designs

J. L. Milovich, P. Amendt, A. Hamza, M. Marinak, H. Robey

July 5, 2006

Twenty-Ninth European Conference on Laser Interaction with Matter
Madrid, Spain
June 11, 2006 through June 16, 2006

Updated October 14, 2003

HIGHLY-RESOLVED 2D HYDRA SIMULATIONS OF DOUBLE-SHELL IGNITION DESIGNS [1]

J. L. Milovich*, P. Amendt*, A. Hamza*, M. Marinak* and H. Robey*

University of California, Lawrence Livermore National Laboratory, Livermore, California 94550

ABSTRACT

Double-shell (DS) targets (Amendt, P. A. *et al.*, 2002) offer a complementary approach to the cryogenic baseline design (Lindl, J. *et al.*, 2004) for achieving ignition on the National Ignition Facility (NIF). Among the expected benefits are the ease of room temperature preparation and fielding, the potential for lower laser backscatter and the reduced need for careful shock timing. These benefits are offset, however, by demanding fabrication tolerances, e.g., shell concentricity and shell surface smoothness. In particular, the latter is of paramount importance since DS targets are susceptible to the growth of interface perturbations from impulsive and time-dependent accelerations. Previous work (Milovich, J. L. *et al.*, 2004) has indicated that the growth of perturbations on the outer surface of the inner shell is potentially disruptive. To control this instability new designs have been proposed requiring bimetallic inner shells and material-matching mid-Z nanoporous foam. The challenges in manufacturing such exotic foams have led to a further evaluation of the densities and pore sizes needed to reduce the seeding of perturbations on the outer surface of the inner shell, thereby guiding the ongoing material science research efforts. Highly-resolved 2D simulations of porous foams have been performed to establish an upper limit on the allowable pore sizes for instability growth. Simulations indicate that foams with higher densities than previously thought are now possible. Moreover, while at the present time we are only able to simulate foams with average pore sizes larger than 1 micron (due to computational limitations), we can conclude that these pore sizes are potentially problematic. Furthermore, the effect of low-order hohlraum radiation asymmetries on the growth of intrinsic surface perturbations is also addressed. Highly-resolved 2D simulations indicate that the transverse flows that are set up by these low-order mode features (which can excite Kelvin-Helmholtz instabilities) are not large enough to offset the overall robustness of our current design.

1. INTRODUCTION

A large body of work (Callahan, D. A. *et al.*, 2006) has been devoted to achieving ignition on the National Ignition Facility (NIF) when operational in 2010. The current ignition plan calls for the use of a cryogenic single shell capsule in the indirect-drive configuration. However, the demands on the laser system (contrast ratios as high as 100:1) and the need for cryogenic preparation and fielding (the triple point of DT is 18.3° K) have motivated a look into complementary designs that may ease these requirements. One such design that is getting renewed attention, is a double-shell (DS) target. As the name indicates, it consists of two concentric shells. The pusher (inner shell) consists of a high-Z material filled with DT fuel at room temperature. Its main function is to limit radiation losses from the burning fuel and to provide prolonged fuel confinement. The inner shell (IS) is supported by a low density foam within a low-Z outer shell (ablator) whose function is to deliver the energy acquired from the absorbed hohlraum x rays to the pusher upon spherical convergence and shell collision. Double shells were proposed in the late 1970's with the introduction of the Apollo targets (Lindl, J. D., 1978). In the 1980's ex-

[1] This work was performed under the auspices of the U.S. Department of Energy by the University of California Lawrence Livermore National Laboratory under contract N° W-7405-ENG-48.

periments designed to verify the predicted performance gave discouraging results and DS were discarded as a possible ignition option. However, the attractiveness of the non-cryogenic preparation and the less demanding laser power requirements motivated a few researchers (Varnum, W. S. *et al.*, 2000; Amendt, P. A. *et al.*, 2002) to revisit these targets using state-of-the-art computational tools. On the other hand, DS targets are susceptible to the growth of interface perturbations excited by either impulsive or time-dependent accelerations since they lack stabilization mechanisms from ablation and density gradients. These instabilities are responsible for the mix between the high-Z IS and the fuel at deceleration onset. This mechanism was considered to be the most dangerous failure mode of DS targets, and a considerable amount of work (Amendt, P. A. *et al.*, 2002) was devoted to reducing it. A different failure path, however, was not identified until later (Milovich, J. L. *et al.*, 2004) when highly-resolved multi-mode simulations revealed that perturbations present on the outer surface of the inner shell were driven Rayleigh-Taylor (RT) unstable by x-ray preheat. The outer surface of the IS ablates due to high-energy x-rays from the hohlraum wall. Contrary to single-shell capsules where the ablated material causally leaves the implosion environment, the ablated outer-shell material gets recollected by the incoming outer-shell through the intervening foam. This "snow-plow" effect sets up a density jump ($\approx$ 4x, and a consequently large Atwood number ≈ 0.7) at the foam-pusher interface in the direction which allows the development of RT instability. The large growth of short wavelength perturbations provides a source of energy for a downward cascade to low-order modes, which are efficient in breaking up the shell and quenching ignition. Figure 1a shows the material contours about 200 ps before the "clean" (no perturbations) 1D peak neutron production time. It is evident that at this time, the IS has disassembled with the subsequent yield $\approx$ 1% YoC [2)]. Alternative designs were proposed to mitigate this instability. Figure 1b shows one of them, consisting of a 40 μm thick Ti tamping layer over the outer surface of the IS. This capsule also suffers from the same instability as the original design, but by introducing the tamping layer we were able to reduce both the Atwood number (≈ 0.3) and the expansion of the outer surface of the pusher ($\approx$ a quarter of its original radius). Thus, the rate and duration of instability growth were reduced. Note that the outer surface of the tamping layer is also subject to the same instability but to a lower extent because of the smaller Atwood number at the tamper-foam interface. The existence of small-scale growth combined with our inability to perform credible simulations to model such finely detailed structures compelled us to resort to a more innovative design. Our criterion was to reduce as much as possible any large density jumps at material interfaces. One obvious approach is to include a suite of tamping layers with intermediate densities between the pusher (Au/Cu) and the foam densities. We gave careful consideration to this design but the growth of large mode-number perturbations was still present, although at a much lower level. A direct extension of this approach, which maximally eliminates the growth of these perturbations, is one in which the pusher itself consists of a variable density/composition between its inner and outer surfaces. To solve the additional problem of having a low-density supporting foam with different material composition we also propose the use of a low-density foam made of the same material as the outer layer of the IS. Current plans call for a bimetallic inner shell ranging from pure Au in the inner surface to pure Cu at the outer surface, supported by a pure-Cu low-density metallic foam. The behavior of this capsule is exhibited in fig. 1c. The 1D-like behavior is remarkably striking. At the time that this target was proposed no demonstrated bimetallic shells able to hold the required pressures were available. Furthermore, metallic foams were just beginning to be investigated but with densities and compositions much higher than required. To date, several major breakthroughs in nano-science based materials have been accomplished and their description is the subject of a companion paper in these proceedings (Amendt *et al.*). The difficulty in making these exotic foams has motivated us to take another look at the required

---

[2)] YoC: (measured yield over clean predicted yield, i.e. one-dimensional simulated yield with no mix

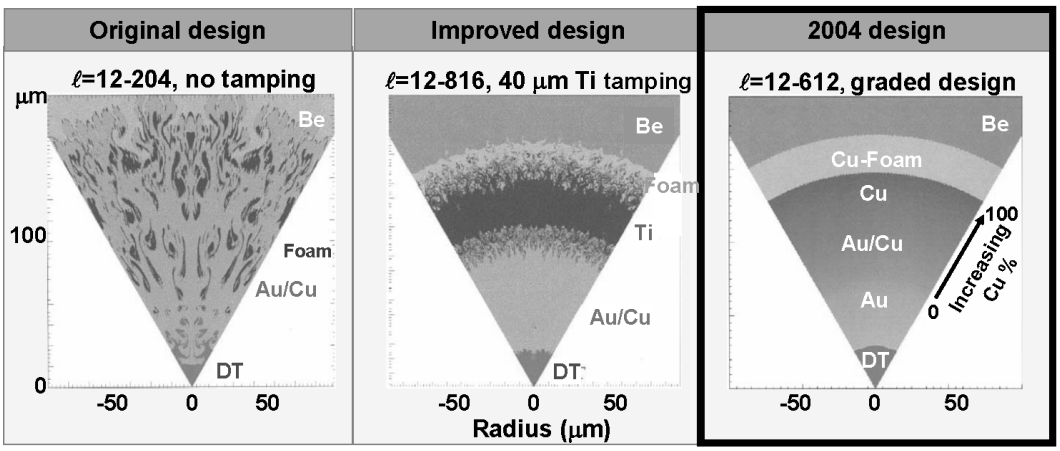

FIGURE 1. Highly-resolved multi-mode computer simulations of a) originally proposed design (Amendt, P. A. *et al.*, 2002) b) modified with 40 μm Ti-tamped inner shell c) optimized design with density graded inner shell and metallic low-density foam.

densities (§3), thereby facilitating the current materials research efforts. Furthermore, our earlier work was based exclusively on the growth of perturbations seeded by surface roughness on the IS. However, foam porosity and roughness are sure to play a role in seeding these instabilities. Previous work (Garbett, W. *et al.*, 2003) concluded that the foam porosity of targets in a recent LANL Omega campaign was the cause of their poor performance. In order to understand the physical mechanisms at play we have begun an ambitious computational program devoted to determining limits on the allowable pore sizes for a successful reduction of instability growth. Our preliminary results indicate that pore sizes larger than 1 μm (which is the lower limit that can be achieved with current computational resources) could be problematic. Also, hohlraum x-ray flux asymmetry must be taken into account. Large, low-mode flux asymmetry (< 2 keV) impinging on the outer shell can impart a sizable perturbation on the pusher after shell collision. Furthermore, low-mode drive asymmetry gives rise to shear flows which can excite Kelvin-Helmholtz (KH) instabilities. The growth of these perturbations provides a seed that can be further enhanced by RT instability. High-resolution simulations are performed to assess the combined effect of both surface roughness and low-mode drive asymmetries (§4). Our results indicate that the current design is able to withstand these asymmetries, and IS integrity is maintained. Furthermore, our simulations show little contribution of shear-flow instabilities to the overall RT growth of small scale perturbations.

2. SIMULATION SETUP

We use the radiation-hydrodynamics code HYDRA to perform capsule-only simulations. A detailed description of the code can be found elsewhere (Marinak, M. M. *et al.*, 2001). Briefly, the code uses an operator splitting technique to couple all the different physical processes: hydrodynamics, heat conduction, and radiation transport. The hydro package is based on a structured mesh and uses the arbitrary Lagrangian-Eulerian (ALE) framework. In our simulations we use the diffusion approximation for both thermal conduction and radiation transport. Equation of state data is obtained in line, by using the QEOS package (More, R. M. *et al.*, 1988). Opacities are obtained from the XSN model (Lokke, W. A. and GRASBERGER, W. H., 1977; Zimmerman, G. B. and MORE, R. M., 1980; More, R. M., 1982) in the local thermodynamic equilibrium approximation. Thermal conductivities use the Lee and More formulas (Lee, Y. T. and MORE, R. M., 1984). As in our previous work (Milovich, J. L. *et al.*, 2004), to avoid excessive numerical dissipation of the largest l-modes we use at least 20 points per wavelength, making our simulations very computationally expensive. Therefore, to effectively use our fi-

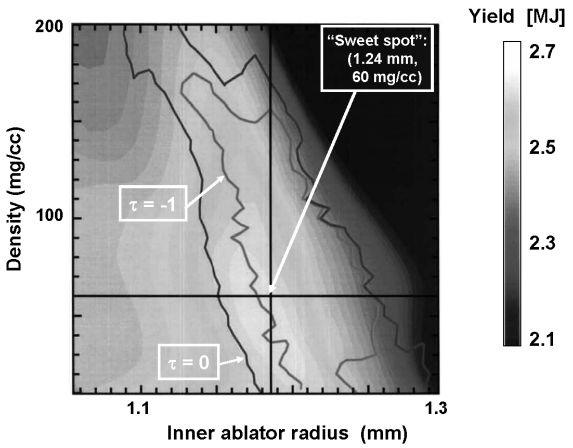

FIGURE 2. Contours of thermonuclear yield vs foam density and ablator thickness. The contours labeled $\tau = 0, -1$ delimit designs with less susceptibility to mix. The cross-hair point indicates the most optimum design with higher yield and less susceptibility to mix.

nite computational resources we resort to capsule-only 2D simulations driven by a frequency-dependent-source (FDS) obtained from a separate low resolution integrated hohlraum simulation. When asymmetries in the radiation source are included (§4) they are also extracted from the same integrated simulation and used to modulate the FDS source in angle.

3. FOAM DENSITY AND POROSITY

The manufacturing of low-density, low-porosity metallic foams is daunting. To aid in this challenging process we have initiated a computational program with the objective of determining limits on the required density and porosity for a successful DS design. To this end, we use the design from fig. 1c and perform numerous 1D simulations to ascertain the most optimum foam density. Figure 2 shows a summary of the results, where we show the contours of the thermonuclear yield (one of the metrics of performance) as a function of foam density and ablator thickness [3)]. To select the best performing target, we also require that our target be robust to the growth of perturbations at the fuel/pusher interface (occurring after deceleration onset). A measure of this is the mix-susceptibility parameter [4)] τ introduced in Amendt, P. A. *et al.*, 2002. A negative value for τ corresponds to less susceptibility to mix and therefore less yield degradation. In fig. 2 we have superimposed the contours of $\tau = 0$ and $\tau = -1$. The "sweet spot" point depicted in fig. 2 corresponds to the best value for foam density and thermonuclear yield. Note that foam density values larger than the optimum are also acceptable and we can entertain designs with foam densities as high as 150 mg/cc if necessary. Though, this may be beneficial for target fabrication, the proximity of these designs to scenarios with positive τ values would leave little margin for error.

Now that we have identified the best operating foam density regime, we look for mechanisms to seed instability. Foam structure such as porosity and foam surface roughness play a role in seeding the dangerous instability shown in fig. 1a. The physical mechanisms can be described as follows. Foam porosity can be thought of as mass irregularities which in turn can be viewed as perturbations onto an otherwise perfectly smooth inner shell. Using this picture, we can evaluate the effective root-mean-square surface roughness produced by a foam of a certain pore size.

[3)] Changing the foam density requires changing the mass of the ablator to achieve maximum energy transfer at shell collision

[4)] The fall-line is the trajectory that material at the fuel-pusher interface would follow in the absence of deceleration. The parameter τ is defined as the difference between the time of peak burn and the time the fall-line reaches the origin, normalized to the full-width half-maximum burn history.

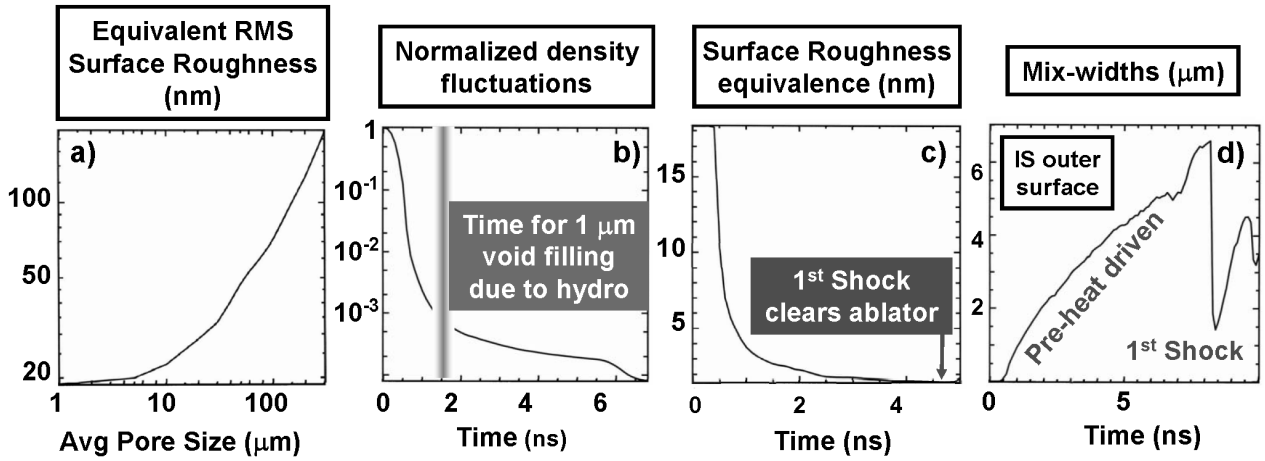

FIGURE 3. Summary of foam simulation: a) equivalent root-mean-square outer shell surface roughness (ESR) as functions of average pore size; b) time variation of the normalized foam density fluctuations due to x ray preheat absorption and homogenization; c) change in the ESR due to x ray preheat absorption; d) inner shell outer surface perturbation seeding due to differential x ray preheat expansion caused by foam surface roughness and porosity

The result of this procedure is exhibited in fig. 3a, where as expected large pore foams have a larger impact. This effect is mitigated, however, by the absorption of high-energy x rays from the high-Z hohlraum walls by the metallic foam. This mechanism aids in reducing the density inhomogeneities existing at scales comparable to the pore-size. Highly-resolved 2D simulations have verified this physical picture. Fig. 3b shows the average density fluctuations within the foam over time. It is clear that density inhomogeneities get reduced by a factor of ≈ 1000 within the first 2 ns (approximately 3 ns before the first shock clears the inner ablator surface). Fig. 3c shows the equivalent inner-shell outer-surface roughness (ESR) predicted by our simulation as a function of time. It is clear that at about 5 ns, the time in which the first shock clears the ablator, the initial ESR is significantly reduced ($\approx$ 20x or $<$ 1 nm). Since surface finishes are within a few tenth of nanometers the effect of foam-porosity alone is not expected to cause any major seeding of perturbations. Foam surface roughness, on the other hand, can be more problematic. Preheat also plays a role here. Exposure of the IS to hard x-rays ablates its outer surface as was shown in Milovich, J. L. *et al.*, 2004. The combined presence of foam surface roughness (which is expected to be within 2-5 μm) and porosity (≈ 1 μm in our simulation) acts to perturb the expansion velocity effectively seeding a perturbation. Due to the kinematic origin of these effects, the root-mean-square size of these perturbations varies linearly with time. This is indicated in fig. 3d where we plot the mix-width at the pusher-foam interface as a function of time. As predicted the perturbation amplitude increases linearly in time and by the time it gets recollected by the incoming shock it has reached a value in excess of 6 μm. Our 2D simulation indicates that such a large initial value perturbation has a significant effect on the performance of the DS target of fig. 1c. The growth of short wavelength perturbations still ensues but it is largely mitigated by our engineered density gradient which helps to keep the IS intact (not shown). However, the down-cascade to larger scales which are able to feed-through to the inner surface causes substantial yield reduction ($\approx$ 10% of the yield obtained in our 1D clean calculations). Reducing the impact of foam structure to alleviate its impact is the matter of current research efforts in nano-materials science at LLNL.

4. RADIATION ASYMMETRIES

A key requirement to achieving ignition in an indirect-drive approach is to control capsule implosion symmetry. To control lower-order radiation asymmetries much effort is devoted to

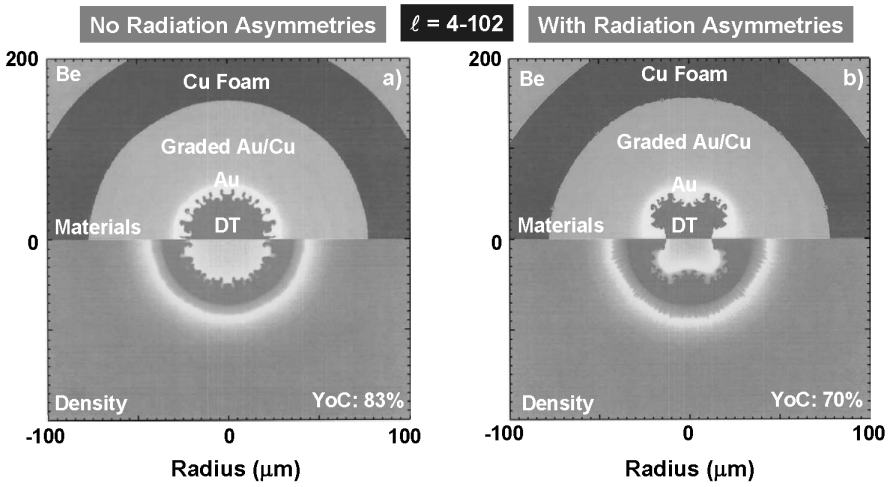

FIGURE 4. Comparison between 2D multi-mode simulation: a) without and b) with radiation asymmetries respectively. Both including modes l=4 to 102

optimizing laser beam pointing as well as the ratio of hohlraum to capsule radius. Even in the best of scenarios the presence of the laser-entrance-holes (LEH) as well as the motion of the laser spots (due to the ablation of the hohlraum wall) throughout the implosion history can give rise to appreciable low-order mode amplitudes. In practice, modes with l-number larger than 10 are successfully smoothed by hohlraum emission and re-absorption while low-order modes with $l = 2, 4$ still remain at levels which need to be addressed for a successful ignition attempt. Modes with $l = 6, 8$ exist at a lower level but they can become troublesome due to mode coupling and RT-growth that can ensue during the implosion history. Furthermore, when instabilities such as the one described in §1 are present, the combined effect needs to be addressed so as to determine and control the potential modes of failure. To this end, we have commenced an intensive campaign to determine the allowable levels of radiation asymmetries to achieve ignition. The major effect of these asymmetries is to set up azimuthal flows. In turn, these flows can give rise to Kelvin-Helmholtz (KH) instabilities. The common stabilizing mechanisms, such as viscosity, are too low to effectively alter the growth rate of these instabilities. Furthermore, even if the rate of growth is small compared to the relevant implosion time, KH growth may seed short-wavelength perturbations that, as we saw earlier, can be further enhanced through RT instabilities.

To address this issue, we have performed several integrated hohlraum simulations to obtain the best laser beam pointings and beam phasing. Due to spot motion a residual asymmetry still remains. Therefore, we extracted the remaining low-order mode radiation asymmetry coefficients as a function of time and used them to modulate our FDS in our capsule-only multi-mode simulations. The results of this exercise are shown in fig. 4 where we compared our calculations without (fig. 4a) and with (fig. 4b) radiation asymmetries at the time of peak neutron production. The first thing to notice is that even in the presence of flux asymmetries we have succeeded in preventing disruption of the inner shell. The major difference with the case shown in fig. 4a is the shape of the fuel cavity, which clearly shows a substantial deformation (for the specifics of this simulation the overall shape corresponds to a negative P_4) mainly due to the high convergence of these targets (about a factor of 30). The influence on the short wavelength perturbations on the other hand appears to be minimal. The growth of perturbations on the outer surface of the inner shell is slightly larger than in Fig. 4a (though imperceptible in the scale of the picture) but still kept in check due to our engineered density gradient inner shell. The mix-width associated only with the small-scale perturbations at the fuel-pusher interface, is also practically unchanged when compared to the case without radiation asymmetries. This indicates minimal seeding from the growth of KH instabilities. However, there is a larger yield degradation which appears to be

split with 50% coming from high-mode mixing and 50% from low-mode radiation asymmetry. Finally, simulations including up to $l = 408$ are currently in progress, but initial results show that the above conclusion remains true.

5. SUMMARY AND CONCLUSIONS

We have performed highly-resolved 2D simulations of double-shell targets proposed as a complementary path to ignition on the NIF. These simulations have identified a new path for the growth of perturbations on the outer surface of the IS of earlier designs that if left uncontrolled would give rise to an inner-shell disruption. To maximally reduce this instability a new design was proposed that consists of a bimetallic graded-density inner-shell supported by a low-density (60 mg/cc) nanoporous metallic foam having the same material composition as the outer layers of the IS. This design showed a remarkable stability to the growth of short wavelength perturbations in ideal simulations, i.e., no foam structure or drive asymmetries. To test further the behavior of this new design under these conditions, we performed highly-resolved simulations that included foam porosity and foam surface roughness. These simulations indicate that the porosity structure that can be imparted onto the surfaces of the IS by the intervening shocks is smoothed out by preheat to a level which is practically negligible by the time the first shock clears the outer shell. Foam surface roughness on the other hand can be more problematic. Preheat is responsible for ablating the outer surface of the inner shell. The foam surface roughness and porosity act to perturb the otherwise uniform expansion velocity. This differential velocity perturbation grows linearly with time reaching large values by the time the shell is recollected by the incoming ablator. This large perturbation gets fed-through to the inner surface with non-negligible yield reduction ($\approx$ 10% YoC). It is worth mentioning that even such large perturbations are stabilized by our engineered bimetallic IS and matching foam to such a degree that the IS remains intact. Finally, the effect of low-mode radiation drive asymmetries on the growth of short-scale surface perturbations is studied. Our simulations indicate that their effect is mainly concentrated to fuel cavity deformation. The shear flow instabilities that arise are not large enough to significantly alter the growth of short-wavelength perturbations. Comparison with simulations with perfectly symmetric drive shows that the contribution to thermonuclear yield degradation from the low-mode drive asymmetries appears to equal the yield reduction from fuel-pusher mix.

6. REFERENCES

1. AMENDT, P. A., COLVIN, J. D., TIPTON, R. E., HINKEL, D. E., EDWARDS, M. J., LANDEN, O. L., RAMSHAW, J. D., SUTER, L. J., VARNUM, W. S., and WATT, R. G., *Phys. Plasmas*, **9**, 2221 (2002).
2. CALLAHAN, D. A., AMENDT, P. A., DEWALD, E. L., HAAN, S. W., HINKEL, D. E., IZUMI, N., JONES, O. S., LANDEN, O. L., LINDL, J. D., POLLAINE, S. M., SUTER, L. J., TABAK, M., and TURNER, R. E., *Phys. Plasmas*, **13**, 056307 (2006).
3. GARBETT, W., GRAHAM, P., and DUNNE, A. M., An assessment of mix in omega double shell capsule implosions, *Proceedings of Third International Conference on Inertial Fusion Science Aplications*, Monterey, CA (2003), pages 126-130.
4. LEE, Y. T., and MORE, R. M., *Phys. Fluids*, **27**, 1273 (1984).
5. LINDL, J. D., "Apollo targets for Nova and KrF-driven reactors", Laser program annual report, ucrl-50055-78, pp. 2-77 to 2-88, Lawrence Livermore National Laboratory, Livermore, CA (1978), unpublished.
6. LINDL, J., *et al.*, *Phys. Plasmas*, **11**, 339 (2004).
7. LOKKE, W. A., and GRASBERGER, W. H., Ucrl-52276, Lawrence Livermore National Laboratory, Livermore, CA (1977).
8. MARINAK, M. M., KERBEL, G. D., GENTILE, N. A., DITTRICH, T. R., and HAAN, S. W., *Phys. Plasmas*, **8**, 2275 (2001).
9. MILOVICH, J. L., AMENDT, P. A., ROBEY, D. H., and MARINAK, M. M., *Phys. Plasmas*, **11**, 1552 (2004).
10. MORE, R. M., *J. Quant. Spectrosc. Radiat. Transfer*, **27**, 345 (1982).
11. MORE, R. M., WARREN, K. H., YOUNG, D. A., and ZIMMERMAN, G. B., *Phys. Fluids*, **31**, 3059 (1988).
12. VARNUM, W. S., *et al.*, *Phys. Rev. Lett.*, **84**, 5153 (2000).
13. ZIMMERMAN, G. B., and MORE, R. M., *J. Quant. Spectrosc. Radiat. Transfer*, **23**, 517 (1980).